1-15-2017

The Iron-Type Nitrile Hydratase Activator Protein Is A GTPase

Natalie Gumataotao
Loyola University Chicago

Karunagala Pathiranage Wasantha Lankathilaka
Marquette University, wasanthalankathilaka.karunagalapathiranage@marquette.edu

Brian Bennett
Marquette University, brian.bennett@marquette.edu

Richard C. Holz
Marquette University, richard.holz@marquette.edu

Accepted version. *Biochemical Journal*, Vol 474, No. 2 (January 15, 2017): pg. 247-258. DOI.

The Iron-Type Nitrile Hydratase Activator Protein Is A GTPase

Natalie Gumataotao
Department of Chemistry and Biochemistry, Loyola University Chicago, Chicago, IL
K.P. Wasantha Lankathilaka
Department of Chemistry, Marquette University, Milwaukee, WI
Brian Bennett
Department of Physics, Marquette University, Milwaukee, WI
Richard C. Holz
Department of Chemistry, Marquette University, Milwaukee, WI

Abstract: The Fe-type nitrile hydratase activator protein from *Rhodococcus equi* TG328-2 (*Re*NHase TG328-2) was successfully expressed and purified. Sequence analysis and homology modeling suggest that it is a G3E P-loop guanosine triphosphatase (GTPase) within the COG0523 subfamily. Kinetic studies revealed that the Fe-type activator protein is capable of hydrolyzing

Biochemical Journal, Vol 474, No. 2 (January 15, 2017): pg. 247-258. DOI.

GTP to GDP with a k_{cat} value of $1.2 \times 10^{-3}\,s^{-1}$ and a K_m value of 40 μM in the presence of 5 mM $MgCl_2$ in 50 mM 4-(2-hydroxyethyl)piperazine-1-ethanesulfonic acid at a pH of 8.0. The addition of divalent metal ions, such as Co(II), which binds to the *Re*NHase TG328-2 activator protein with a K_d of 2.9 μM, accelerated the rate of GTP hydrolysis, suggesting that GTP hydrolysis is potentially connected to the proposed metal chaperone function of the *Re*NHase TG328-2 activator protein. Circular dichroism data reveal a significant conformational change upon the addition of GTP, which may be linked to the interconnectivity of the cofactor binding sites, resulting in an activator protein that can be recognized and can bind to the NHase α-subunit. A combination of these data establishes, for the first time, that the *Re*NHase TG328-2 activator protein falls into the COG0523 subfamily of G3E P-loop GTPases, many of which play a role in metal homeostasis processes.

Introduction

Nitrile hydratases (NHases, EC 4.2.1.84) are metalloenzymes that catalyze the hydration of nitriles to their corresponding higher value amides under mild conditions (room temperature and physiological pH).[1,2] NHases have attracted substantial interest as biocatalysts in preparative organic chemistry and are used in the large scale industrial production of acrylamide[1,3–6] and nicotinamide.[7] X-ray crystallographic studies indicate that they are $\alpha_2\beta_2$ heterotetramers with an active site consisting of three cysteine residues, two amide nitrogens, a water molecule, and either a nonheme Fe(III) ion (Fe-type) or a noncorrin Co(III) ion (Co-type).[8,9] Two of the active site cysteine residues are post-translationally modified to cysteine sulfinic acid ($-SO_2H$) and cysteine sulfenic acid (–SOH), yielding an unusual metal co-ordination geometry, termed a 'claw-setting'. Oxidation of the equatorial Cys residues is required for catalytic activity.[10,11]

Even though the structures of Fe- and Co-type NHases are very similar, Fe-type NHases are specific for Fe(III), whereas Co-type NHases are specific for Co(III).[8] Several open reading frames have been identified just downstream from the structural α- and β-subunit genes in NHases, and one of these genes has been proposed to function as an activator protein (Figure 1).[12–14] The prevailing dogma is that both Co- and Fe-type NHase enzymes require the co-expression of an activator protein to be fully metallated, post-translationally modified, and fully functional.[12–14] While Co- and Fe-type NHase enzymes share high sequence similarity, their respective activator proteins are different in size and share little to no sequence identity,

Biochemical Journal, Vol 474, No. 2 (January 15, 2017): pg. 247-258. DOI.

suggesting that the mechanism of metallocenter assembly is probably different between Co- and Fe-type NHase enzymes.[15–17]

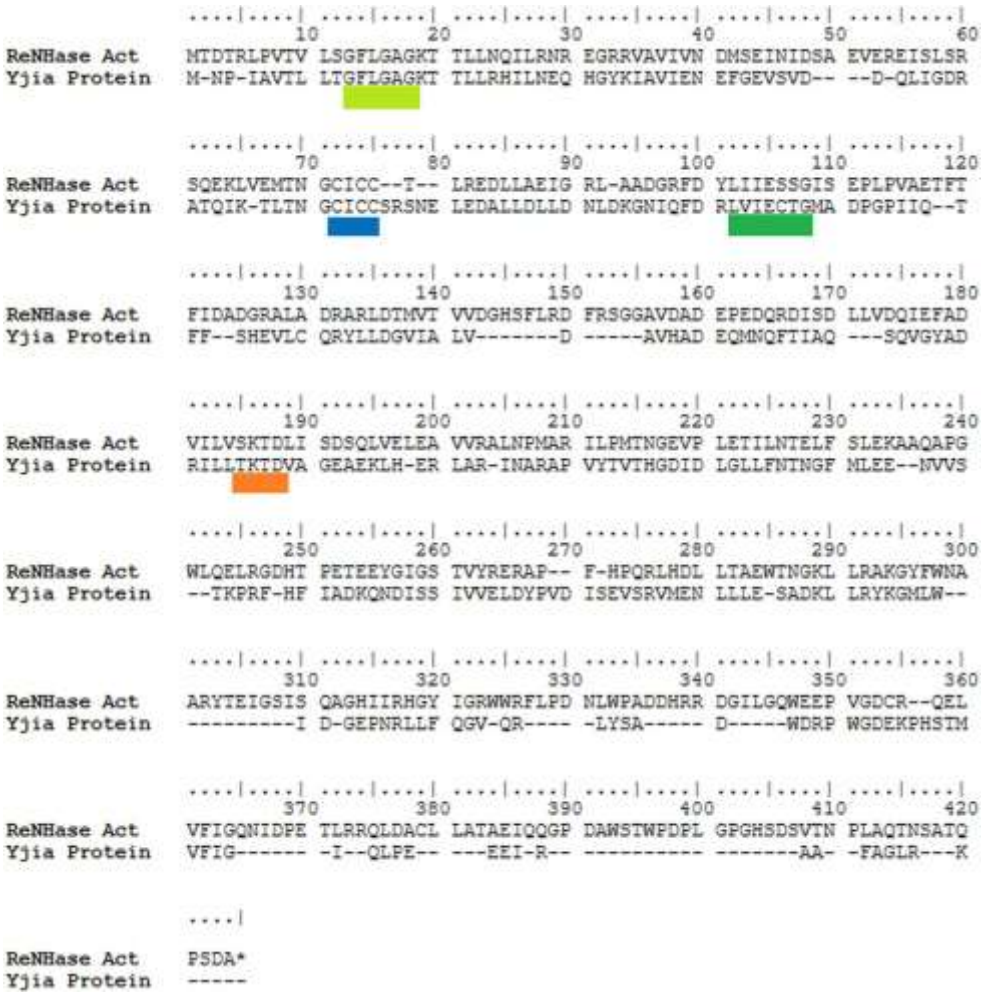

Figure 1. Sequence alignment of Yjia and the Fe-type *Re*NHase TG328-2 activator protein.
The alignment shows (light green — Walker A motif; dark green — Walker B motif; blue — metal-binding motif; orange — guanine-binding motif) shows conserved regions common to P-loop GTPases that are probably responsible for GTPase activity of the proteins.

Activator proteins (ε) for cobalt-type NHases are small (~15 kDa) and have a significant sequence identity with the NHase β-subunit.[18,19] The Co-type activator protein for the low-molecular-weight NHase from *Rhodococcus rhodochrous* J1 has been shown to form an $\alpha\varepsilon_2$ complex, which was proposed to bind Co(II) and insert it into the apo-$\alpha_2\beta_2$ NHase complex via a 'self-subunit swapping' mechanism.[17] The Co-type activator protein was also proposed to

facilitate the oxidation of the two active site Cys residues. On the other hand, Fe-type NHase activator proteins are ~45 kDa and contain a highly conserved cysteine-rich (CXCC) motif that is a known metal-binding site in other metallochaperones, such as COX17 (copper) and the Hyp proteins (nickel).[20,21]

To date, no Fe-type activator protein has been purified or characterized. As such, no molecular level evidence exists regarding the structure or function of the Fe-type NHase activator protein in the biosynthesis of Fe-type NHase enzymes. Therefore, we set out to purify the Fe-type activator from *Rhodococcus equi* TG328-2. The gene encoding the activator protein was synthesized with optimized *E*scherichia *coli* codon usage and heterologously overexpressed in *E. coli* as a maltose-binding protein (MBP)–protein construct. The resulting protein binds divalent metal ions and can function as a guanosine triphosphatase (GTPase). The hydrolysis of GTP by a Fe-type NHase activator protein is a previously unknown role that may be connected to NHase metallocenter assembly.

Materials and methods

Materials

2-amino-2-hydroxymethyl-propane-1,3-diol (Tris–HCl), and 4-(2-hydroxyethyl)piperazine-1-ethanesulfonic acid (HEPES) were obtained from Sigma–Aldrich. Oligonucleotides were obtained from Integrated DNA Technologies, Inc. All other reagents were purchased commercially and were of the highest purity available.

Plasmids

The plasmid expressing the Fe-type NHase from *R. equi* TG328-2 (*Re*NHase TG328-2) was kindly provided by Prof. Uwe Bornscheuer (University of Greisfwald).[22] The original plasmid had the NHase α,β, and activator genes in tandem. NHases are typically expressed when the genes for the α- and β-subunits and the activator are co-expressed on separate, complementary plasmids. Therefore, the α- and β-subunit and activator genes from the original plasmid were isolated and subcloned into pET-21a$^+$ and pET-28a$^+$ plasmids, respectively. The

Biochemical Journal, Vol 474, No. 2 (January 15, 2017): pg. 247-258. DOI.

activator was removed from the pET-28a$^+$ plasmid and ligated into pMCSG9 forming the *Re*NHase(e)–MBP–His_6 plasmid containing a tobacco etch virus (TEV) protease cleavage site between MBP and the *Re*NHase (ε) protein.[23] All plasmid sequences were confirmed using automated DNA sequencing at the University of Chicago Cancer Research Center DNA sequencing facility.

Expression and purification of the recombinant ReNHase activator protein

The *Re*NHase (ε)–MBP–His_6 plasmid containing the Fe-activator protein was transformed into BL21(DE3) (Stratagene) cells for gene expression. A single colony from the transformation was used to inoculate a 50 ml LB Miller culture containing 50 μg/ml kanamycin and allowed to grow at 37°C with constant shaking overnight. This culture was used to inoculate 3 l of LB Miller culture containing kanamycin (50 μg/ml) and ampicillin (100 μg/ml). Cells were allowed to grow at 37°C with constant shaking until an optical density of ∼0.8–1.0 at 600 nm was reached. The culture was cooled to 18°C and induced with 0.1 mM isopropyl-β-d-1-thiogalactopyranoside and then shaken for 16 additional hours at 18°C.

Cells were pelleted by centrifugation at 5000 × ***g*** for 5 min and resuspended in 50 mM sodium phosphate buffer (pH 8.0) containing 300 mM NaCl, 10% glycerol, and 10 mM imidazole at a ratio of 3 ml/g of cells. Cells were lysed by ultrasonication (Misonix Sonicator 3000) in 30 s increments for 4 min at 21 W. Cell lysate was separated from cell debris by centrifugation for 40 min at 10 000 × ***g***. Cell lysate was purified using immobilized metal affinity chromatography (IMAC) on a GE ÄKTA Fast Protein Liquid Chromatography (FPLC) system at 4°C. The protein was eluted from the nickel nitrilotriacetic acid (Ni-NTA) column (100 mg protein/5 ml column) with a linear gradient (0–100%) of a high imidazole content buffer [50 mM NaH_2PO_4 (pH 8.0), 300 mM NaCl, 10% glycerol, and 500 mM imidazole] at a flow rate of 1 ml/min.

Fractions containing the Fe-type activator protein were treated with His_6-tagged TEV protease (5% w/w) and 2 mM dithiothreitol and stirred gently overnight at 4°C. Cleaved protein was purified with IMAC by eluting unbound protein with 100% of a 10 mM imidazole buffer

Biochemical Journal, Vol 474, No. 2 (January 15, 2017): pg. 247-258. DOI.

solution. The protein was then concentrated to 2 ml and loaded onto a 25 ml DEAE-Sepharose (diethylaminoethyl) column equilibrated with anion exchange buffer A [10 mM Tris (pH 8.0) and 10 mM NaCl]. The protein was eluted in a stepwise gradient at 50% of buffer B [10 mM Tris (pH 8.0) and 500 mM NaCl]. The purified protein was then buffer-exchanged using an Amicon centrifugal concentrator (Millipore) into 50 mM HEPES (pH 8.0) and 300 mM NaCl.

Approximately 5 mg/l purified activator protein per liter of culture was obtained. The protein precipitated upon cleavage of the MBP tag, so optimal conditions for solubilization were determined by employing a solubility screen[24] providing optimal conditions of 50 mM HEPES (pH 8.0), 300 mM NaCl, and 10% glycerol. Under these conditions, the activator protein was stable at 4°C for several days. Purification of the activator was confirmed by sodium dodecyl sulfate–polyacrylamide gel electrophoresis. A Bradford assay was performed at 595 nm against bovine serum albumin standards to determine protein concentration.

Nucleotide triphosphatase activity measurement

Nucleotide triphosphatase (NTPase) activity was assayed in triplicate for three separate purifications, using a malachite green assay at NTP [GTP, adenosine triphosphate (ATP), or uridine triphosphate (UTP)] concentrations ranging from 0.05 to 1 mM and Fe-activator protein concentrations of 1–3 μM in 50 mM HEPES (pH 8.0) and 5 mM $MgCl_2$ at 37°C for 5–240 min.[25] The reaction was quenched by the addition of 375 μl of malachite green (2.6 mM malachite green, 1.5% ammonium molybdate, and 0.2% Tween 20), incubated at room temperature for 1 min followed by the addition of sodium citrate to a final concentration of 3.5 mM. The absorbance was measured at 630 nm on a BioTek Synergy 2 Multimode microplate reader and compared with a prerecorded calibration curve. One unit of enzymatic activity is defined as the amount of enzyme catalyzing the formation of 1 μmol min^{-1} PP_i. Error values were determined by averaging all kinetic determinations for each NTP.

Biochemical Journal, Vol 474, No. 2 (January 15, 2017): pg. 247-258. DOI.

Metal analysis

Inductively coupled plasma atomic emission spectroscopy (ICP-AES) analysis was conducted at the Integrated Molecular Structure Education and Research Center (IMSERC) at Northwestern University. All glassware was washed with 1 M HNO_3 prior to use and all buffers were demetallated by using a Chelex-100 column. Purified activator protein was digested in a 5% nitric acid (HNO_3) solution for 15 min at 70°C. The digested protein was filtered through a 0.2 μm Supor membrane (Whatman). The filtered samples were analyzed for iron (238.204 and 259.940 nm), nickel (230.299 and 231.604 nm), and zinc (202.548 and 213.857 nm).

Electronic absorption spectra

Electronic absorption spectra were recorded on a Shimadzu UV-2600 spectrophotometer equipped with a TCC-240A temperature-controlled cell holder. Spectra of the Fe-type activator protein, in 50 mM HEPES (pH 8.0), 300 mM NaCl, and 10% glycerol, were obtained at 25°C in a 1 cm quartz cuvette.

Isothermal titration calorimetry

Isothermal titration calorimetry (ITC) measurements were carried out on a MicroCal ITC200 system. The Fe-type activator protein was incubated with 10 mM ethylenediaminetetraacetic acid (EDTA) in the presence of 20 mM tris(2-carboxyethyl)phosphine (TCEP), used as a reducing agent, at 4°C anaerobically for 24 h in degassed 50 mM HEPES buffer (pH 7.5). The EDTA was removed by dialysis using, at minimum, four buffer exchanges of 50 mM Chelex-treated HEPES buffer at a pH of 7.5. Individual Fe-type activator protein and Co(II) solutions were prepared by diluting stock enzyme or Co(II) solutions with degassed 50 mM Chelex-treated HEPES buffer (pH 7.5) containing 2 mM TCEP and incubated at 4°C for 24 h. The enzyme solution (50 μM) was placed in the calorimeter cell and stirred at 750 rpm to ensure rapid mixing. Typically, 2 μl of Co(II) titrant (500 μM) was delivered over 2 s with a 3 min interval between injections to allow for complete equilibration. Each titration was continued to >2 equiv. of added Co(II) to ensure that no additional complexes were formed with excess

Biochemical Journal, Vol 474, No. 2 (January 15, 2017): pg. 247-258. DOI.

titrant. A background titration, consisting of the identical titrant solution but only the buffer solution in the sample cell, was subtracted from each experimental titration to account for heat of dilution.

Association constants (K_b) were obtained by fitting these data, after subtraction of the background heat of dilution, via an interactive process using the Windows-based Origin software package supplied by MicroCal. This software package uses a nonlinear least-squares algorithm, which allows the concentrations of titrant and the sample along with the heat flow per injection to be fit to an equilibrium binding equation. The K_b value, enzyme–metal stoichiometry (n), and the change in enthalpy ($\Delta H°$) were allowed to vary during the fitting process. The association constant K_b and the enthalpy change ΔH were used to calculate ΔG and ΔS using the Gibbs-free energy relationship (eqn 1):

$$\Delta G^\circ = -RT \ln[K_b] = \Delta H^\circ - T\Delta S^\circ \quad (1)$$

where $R = 1.9872$ cal mol^{-1} K^{-1}. T is temperature in K. The relationship between K_b and K_d is defined as

$$K_d = \frac{1}{K_b} \quad (2)$$

Circular dichroism

A 3 μM sample of purified activator was prepared in 10 mM sodium phosphate (pH 7.5). Spectra were collected from 190 to 260 nm on samples in a 1 mm path-length quartz cell on an Olis DSM circular dichroism (CD) spectrometer. The program CDSSTR (Birkbeck College DICHROWEB reference set 4) was used to analyze the secondary structure of the activator.[26,27] CD spectra were also recorded of the Fe-activator protein in the presence of GTP, ATP, GDP, Mg(II), or Co(II).

Homology modeling

The sequence of the *Re*NHase TG328-2 Fe-activator protein was submitted to SWISS-MODEL.[28–30] A protein database (PDB) blast search identified the YjiA protein (PDB: 1NIJ) as the best template

Biochemical Journal, Vol 474, No. 2 (January 15, 2017): pg. 247-258. DOI.

structure. The resulting homology model was exported to Deepview Swiss PDB Viewer for further refinement and model validation.[31] ProCheck[32] and Verify 3D[33] were run in order to validate the homology model. The Ramachandran plot of the *Re*NHase TG328-2 activator protein homology model revealed that only 1.5% of the structure is in a disallowed region. That combined with a QMEAN score of 0.506 indicates that the model is a reasonable predictive tool.

Results and discussion

Expression of the ReNHase TG328-2 activator protein

A major limitation in examining the proposed metallochaperone properties of a Fe-type NHase activator protein is the lack of an expression system that provides ample amounts of a soluble form of the protein. We have overcome these issues by subcloning the *Re*NHase TG328-2 activator gene into the pMCSG9 plasmid, which contains an N-terminal TEV protease cleavage site followed by MBP and a His_6 tag. The MBP was incorporated to aid protein folding during expression, whereas the His_6 tag allows rapid purification via IMAC. This plasmid was then transformed into BL21(DE3) (Stratagene) cells for protein expression. Purification using IMAC provided ~5 mg of protein per liter of cell culture. The MBP tag was cleaved from the activator using TEV protease with a His_6 tag. Upon cleavage of the MBP tag, the *Re*NHase TG328-2 activator protein was precipitated. Therefore, optimal conditions for stabilization of the activator were determined by employing a solubility screen, which indicated that the protein is soluble in 50 mM HEPES (pH 8.0), 300 mM NaCl, and 10% glycerol. Under these conditions, the activator protein was stable at 4°C for several days.

Sequence analysis

A BLAST search on the *Re*NHase TG328-2 activator protein sequence revealed elements consistent with metal trafficking and GTPase activities.[15] Specifically, there is significant similarity between the *Re*NHase TG328-2 activator protein and the COG0523 subgroup of the G3E family of P-loop GTPases. COG0523 constitutes a diverse group of proteins with unknown function and wide distribution, while

Biochemical Journal, Vol 474, No. 2 (January 15, 2017): pg. 247-258. DOI.

the other three G3E family subgroups contain proteins known to be involved in metalloenzyme homeostasis such as HypB, UreG, and MeaB/ArgK.[15] Structural information for proteins within the COG0523 subgroup is limited to the YjiA protein.[34,35] Alignment of the *Re*NHase TG328-2 activator protein sequence with the Yija protein reveals that it shares broad sequence similarity (31% sequence identity and 49% similarity) and a highly conserved cysteine-rich (CXCC) metal-binding motif (Figure 1).[21] Like the YjiA protein, the Fe-type *Re*NHase TG328-2 activator protein also contains a P-loop (Walker A motif), which characteristically binds the triphosphate group of GTP, and a Walker B motif that is the site of magnesium binding.[34] The presence of these motifs suggests that the *Re*NHase TG328-2 activator protein may possess GTPase activity, which has heretofore never been proposed for an iron-type NHase activator protein.

GTPase activity

GTPase activity was examined by quantifying free phosphate generated from GTP by reaction of a 1–3 μM sample of the *Re*NHase TG328-2 activator protein in 50 mM HEPES and 5 mM $MgCl_2$ at a pH of 8.0 using a malachite green assay (Table 1). Kinetic analysis reveals that the *Re*NHase TG328-2 Fe-type activator can, in fact, hydrolyze GTP with a k_{cat} value of 1.2×10^{-3} s^{-1} and a K_m value of 48 μM (k_{cat}/K_m of 30 s^{-1} M^{-1}); these parameters are comparable with those for related GTPases such as the YjiA ($k_{cat} = 6 \times 10^{-3}$ s^{-1}), YeiR ($k_{cat} = 3 \times 10^{-3}$ s^{-1}), and Ras ($k_{cat} = 3.4 \times 10^{-4}$ s^{-1}) proteins.[34,36,37] The hydrolysis of GTP by the *Re*NHase TG328-2 activator protein is a previously unknown activity and may play a role in NHase metallocenter assembly.

Table 1 Kinetic data for the *Re*NHase TG328-2 activator NTPase activity toward NTP

NTP	**k_{cat} (s^{-1})**	**K_m (μM)**	**k_{cat}/K_m (s^{-1} M^{-1})**
GTP	$(1.2 \pm 0.5) \times 10^{-3}$	40 ± 20	30 ± 20
GTP + cobalt	$(3.1 \pm 1.3) \times 10^{-3}$	170 ± 80	20 ± 10
ATP	$(1.0 \pm 0.2) \times 10^{-3}$	70 ± 30	13 ± 9
UTP	$(3.2 \pm 0.5) \times 10^{-4}$	90 ± 20	4 ± 1

Hydrolytic activity toward ATP and UTP was also examined to determine if the *Re*NHase TG328-2 activator protein is selective for GTP. Kinetic analysis revealed that the *Re*NHase TG328-2 activator

Biochemical Journal, Vol 474, No. 2 (January 15, 2017): pg. 247-258. DOI.

protein is capable of hydrolyzing ATP with a k_{cat} of 1.0×10^{-3} s^{-1} and a K_m of 70 μM, providing a catalytic efficiency k_{cat}/K_m of 13 s^{-1} M^{-1}, whereas UTP exhibits a k_{cat} value of 3.2×10^{-4} s^{-1} and a K_m of 90 μM, providing a catalytic efficiency k_{cat}/K_m of 4 s^{-1} M^{-1} (Table 1). Although the rate of ATP hydrolysis is nearly identical with GTP, the K_m value increased by nearly two-fold. Therefore, based on catalytic efficiencies, the *Re*NHase TG328-2 activator protein prefers GTP, but is capable of hydrolyzing ATP and UTP.

GTP hydrolysis catalyzed by GTPases can be increased by as much as 10^5 by GTPase effector proteins or cofactors, such as divalent metal ions.[38] The addition of Co(II) as a nonoxidizable divalent metal ion probe for Fe(II) to the *Re*NHase TG328-2 activator protein in 50 mM HEPES and 5 mM $MgCl_2$ at a pH of 8.0 doubled the observed rate of GTP hydrolysis but somewhat disrupted GTP binding, reducing the k_{cat}/K_m value from 30 to 20 s^{-1} M^{-1} (Table 1). A similar finding was obtained for the YjiA protein in the presence of Co, which reduced the k_{cat}/K_m value six-fold to 2.3 s^{-1} M^{-1}.[34] On the other hand, the addition of Zn(II) to the YeiR protein enhanced both k_{cat} and K_m, resulting in an eight-fold increase in k_{cat}/K_m.[36] The observed four-fold increase in the GTP K_m value upon the addition of Co(II) to the *Re*NHase TG328-2 activator protein suggests that, unlike typical GTPases, the activator protein does not probably require accessory proteins to release GDP as GTPases typically exhibit GTP affinities in the picomolar to nanomolar range.[37] Taken together, these data support the hypothesis that GTPase activity is related to divalent metal binding and, thus, metal homeostasis in NHase proteins.

Divalent metal-binding properties

Interestingly, the *Re*NHase TG328-2 activator protein contained no detectable iron, zinc, or nickel by ICP-AES even though it contains a cysteine-rich motif, which was proposed to be the metal-binding site. The lack of bound metal ions is probably the result of IMAC purification as >50 mM imidazole is used. Given the effect of divalent metal ions on the observed GTPase activity and the presence of the CXCC metal-binding motif, the divalent metal-binding properties of the *Re*NHase TG328-2 activator protein were investigated using Co(II) as a spectroscopic probe since Fe(II) exhibits no observable bands within

Biochemical Journal, Vol 474, No. 2 (January 15, 2017): pg. 247-258. DOI.

the visible absorption region, whereas the position and molar absorptivities of Co(II) d–d bands reflect the co-ordination number and geometry of the metal ions.[39,40] UV–Vis spectra of 1 equiv. of Co(II) added to a 1 mM solution of the *Re*NHase TG328-2 activator protein at 25°C in 50 mM HEPES, 300 mM NaCl, and 10% glycerol at a pH of 7.5 resulted in an increase in absorption at ~530 nm with a normalized ε_{530} of ~90 M^{-1} cm^{-1} (Figure 2). The molar absorptivity and position of this band suggest stoichiometric binding of Co(II) to the Fe-type activator protein in a distorted five-co-ordinate geometry. A significant increase in absorption at 310 nm is also observed but no distinct band is observable. Such absorptions are characteristic of an S → Co(II) ligand-to-metal charge transfer band, which is indicative of consistent with a Co(II)–*S*-thiolate interaction.

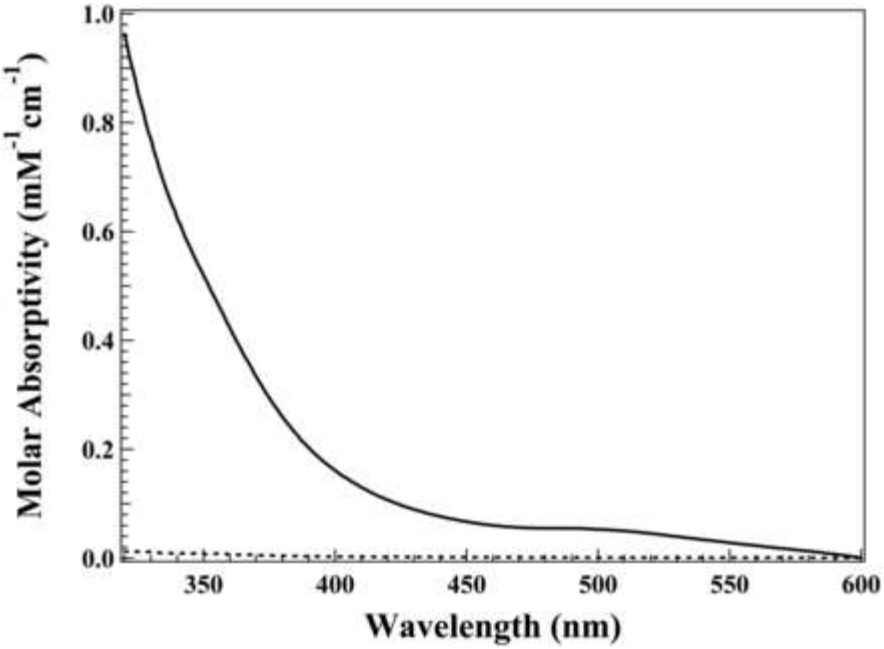

Figure 2. Electronic absorption spectra of the apo-*Re*NHast TG328-2 activator protein and the Co(II) form.
Electronic absorption spectra of the apo-*Re*NHase TG328-2 activator proteins were buffered in 50 mM HEPES, pH 8.0, 300 mM NaCl, and 10% glycerol and spectra collected at 25°C.

ITC measurements on the *Re*NHase TG328-2 activator protein were carried out on a MicroCal iTC200 ultrasensitive titration calorimeter at 25 ± 0.2°C (Figure 3). The best fits obtained for the *Re*NHase TG328-2 activator protein provided an *n* value of 0.87 ± 0.02 and a K_d value of 2.9 ± 0.2 μM. The binding of Co(II) by the *Re*NHase

Biochemical Journal, Vol 474, No. 2 (January 15, 2017): pg. 247-258. DOI.

TG328-2 activator protein is exothermic ($\Delta H = -22.0 \pm 0.8$ kcal mol^{-1}) and entropically driven ($\Delta S = 48.5 \pm 0.5$ cal mol^{-1} K^{-1}). As a control, Co(II) was titrated into EDTA-treated *Re*NHase TG328-2 activator protein in the absence of TCEP. No binding above the heat of dilution was observed, indicating that the reduction in a disulfide bond is required for divalent metal binding. The related YjiA protein binds 1 equiv. of Co(II) with a K_d of 2.0 μM, indicating that Co(II) binds to the *Re*NHase TG328-2 activator protein in a similar fashion to YjiA.

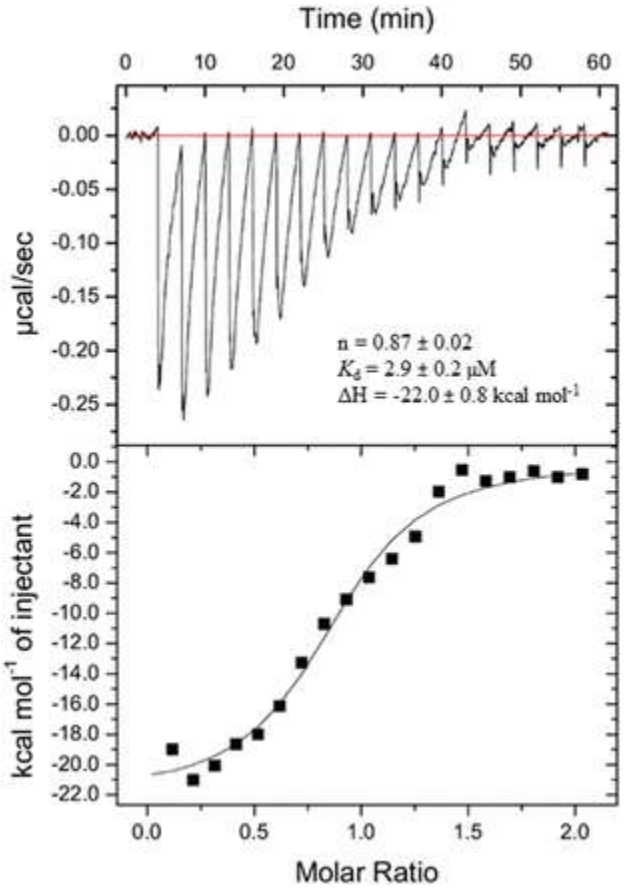

Figure 3. ITC data for Co(II) binding to the *Re*NHase TG328-2 activator protein in degassed 50 mM HEPES buffer (pH 7.5) and 20 mM TCEP, at 4°C.
The activator solution (50 μM) was stirred at 750 rpm while adding 2 μl of Co(II) titrant (500 μM) delivered over 2 s with 3 min intervals between injections.

CD studies

CD spectra were recorded for the *Re*NHase TG328-2 activator protein in the absence and presence of GTP, GDP, Mg(II), and divalent metals ions (Figure 4A,B). The relative secondary structure

Biochemical Journal, Vol 474, No. 2 (January 15, 2017): pg. 247-258. DOI.

deconvolution from the CD spectrum of the as-purified *Re*NHase TG328-2 activator protein resulted in 38% α-helix and 17% β-sheet (Table 2), similar to the YjiA protein (22% α-helix and 26% β-sheet). As is common with GTPases,[41] the addition of GTP, under saturating GTP concentrations, or GDP to the *Re*NHase TG328-2 activator protein significantly altered the secondary structure (Figure 4A and Table 2); a marked decrease in α-helical character and an overall increase in disorder were observed in both cases, though the secondary structures with GTP and GDP, respectively, were distinguishable from the CD spectra. The observed conformational change upon GTP or GDP binding to the *Re*NHase TG328-2 activator protein is probably related to the interconnectivity of these cofactor binding sites. These data indicate a conformational change upon GTP binding and its hydrolysis to GDP, which is common for small GTPases.[41]

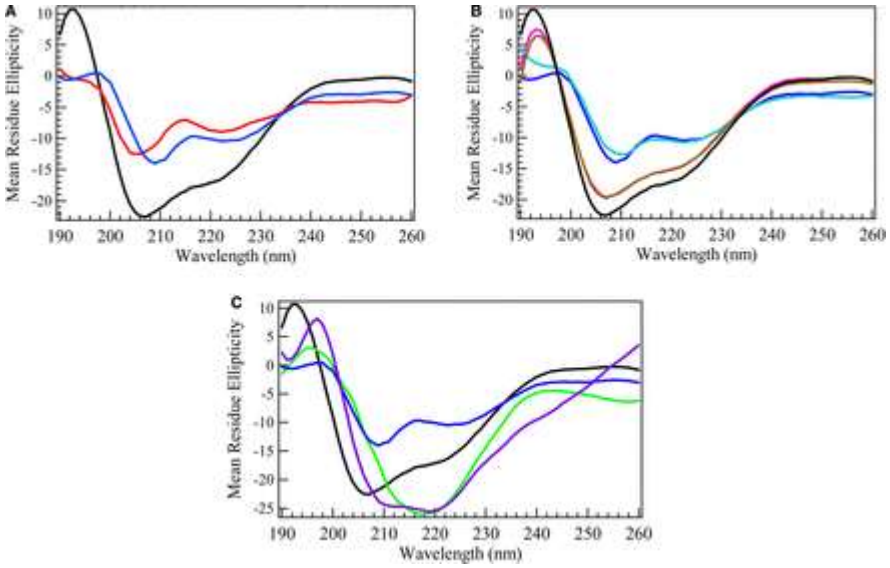

Figure 4. CD spectra of ReNHase activator protein in bound and unbound forms. CD spectra of (**A**) 3 μM *Re*NHase TG328-2 activator protein in 10 mM sodium phosphate buffer at a pH of 7.5 in the absence (black) and presence of GTP (blue) and GDP (red). CD spectra of 3 μM *Re*NHase TG328-2 activator protein was prepared in 10 mM sodium phosphate buffer at a pH of 7.5 in the presence of (**B**) Co(II) (pink), Mg(II) (brown), GTP + Mg(II) (light blue) and (**C**) ATP (green), UTP (purple) and spectra were collected in the 190 to 260 nm on samples in a 1 mm path-length quartz cell.

Biochemical Journal, Vol 474, No. 2 (January 15, 2017): pg. 247-258. DOI.

Table 2 Calculated percentages of secondary structure of free and bound *Re*NHase TG328-2 Fe activator derived from CD data using the CDSSTR algorithm

Sample	α-Helix (%)	β-Sheet (%)	Random coil (%) (T + U)
Activator	38	17	46
GTP	20	27	53
GDP	8	30	62
Co(II)	31	30	38
Mg(II)	31	29	39
Mg(II) + GTP	34	32	49
ATP	45	26	30
UTP	50	23	26

Abbreviations: T, turns; U, unordered.

As the *Re*NHase TG328-2 activator protein is a probable metallochaperone, CD spectra were recorded at a pH of 7.5 in 10 mM sodium phosphate buffer in the presence of 1 equiv. of Co(II) (Figure 4B). No significant conformational change was observed by CD upon the addition of either Co(II) or Mg(II) to *Re*NHase TG328-2 activator protein under conditions where binding is expected. Furthermore, the addition of Mg(II) had no effect on the secondary structure of the GTP-bound protein. The nucleotide, therefore, appears to be the sole candidate for conformational change, other than perhaps interaction with the NHase α-subunit in any conceivable GTP-dependent mechanism for metal trafficking by the *Re*NHase TG328-2 activator protein. Intriguingly, ATP and UTP elicited a conformational change in marked contrast with those of GTP and GDP, in which a marked *increase* in the amount of α-helical structure was evident (Figure 4C). Given that ATP and UTP are hydrolyzed with reasonable efficiency relative to GTP, these data indicate that the conformational change *per se* is probably unconnected with NTPase activity. We speculate that the conformational change is, therefore, important in GTP-dependent iron trafficking and would expect, perhaps, that the hydrolysis of ATP and UTP would not similarly enhance iron trafficking.

Homology model

Currently, no three-dimensional X-ray crystal structure exists for an Fe-type NHase activator protein; therefore, a homological model was developed using the X-ray crystal structure of the Yjia protein (PDB: 1NIJ) as the template (Figure 5A). The resulting model was

Biochemical Journal, Vol 474, No. 2 (January 15, 2017): pg. 247-258. DOI.

validated by the ProCheck and Verify 3D software. The Ramachandran plot of the *Re*NHase TG328-2 activator protein homology model revealed that only 1.5% of the structure is in a disallowed region. That combined with a QMEAN score of 0.506 indicates that the model is a reasonable predictive tool. The homology model of the *Re*NHase TG328-2 Fe-activator protein includes Walker A and Walker B motifs located on an α-helix and adjacent loop region, respectively, characteristic of typical GTPases. Three of the four residues of the DxxG Mg(II)-binding and GTP γ-phosphate-co-ordinating motif are located on a β-sheet, with the last residue on a loop. In addition, an SKTD sequence, similar to the NKED guanine-binding motif common to GTPases, is adjacent to the Walker A-binding site. Finally, the presumed metal-binding (CXCC) motif is located on a β-sheet that is adjacent to the Walker B motif. Two of the Cys residues (C74 and C72) reside on the same side of the β-sheet, suggesting that these two Cys residues can possibly form a disulfide bond. Since the divalent metal-binding site, Mg(II), and GTP-binding sites all reside in a row, this model suggests that there may be some interconnectivity of these cofactor binding sites.

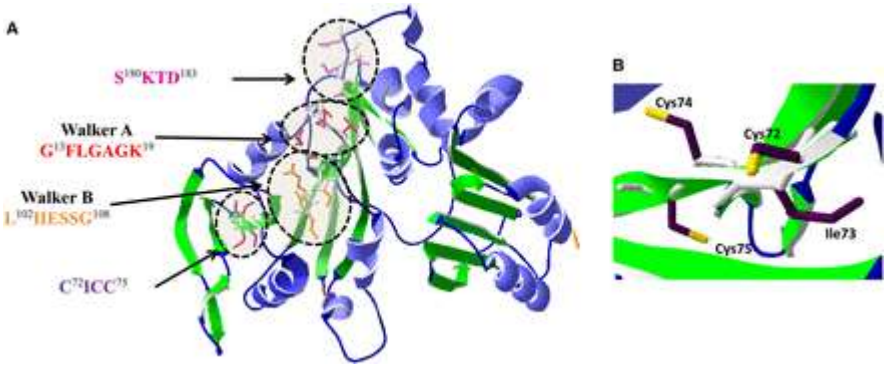

Figure 5. Homology model for the *Re*NHase TG328-2 activator.
The residues making up the Walker A and B motifs highlighted along with the proposed thiolate metal-binding site and the guanine-binding motif. (**B**) An expanded view of the CXCC metal-binding site where it is clear that two of the cysteine residues (Cys 72 and Cys 74) are on the same side of the β-sheet.

Conclusion

An Fe-type NHase activator protein has been expressed and purified for the first time. Sequence analysis suggests the presence of a cysteine-rich divalent transition metal ion-binding motif and distinct GTPase motifs. Construction of a homology model, based on the

Biochemical Journal, Vol 474, No. 2 (January 15, 2017): pg. 247-258. DOI.

related Yjia protein, suggests that a majority of the key residues and sequences for metal-binding and GTPase activity are found on flexible loops, while the proposed divalent metal-binding site is located on a β-sheet adjacent to the Walker B motif. Kinetic studies indicate that the *Re*NHase TG328-2 activator protein exhibits GTPase activity and the addition of divalent metal ions such as Co(II) accelerated the rate of GTP hydrolysis, suggesting that GTP hydrolysis is potentially connected to the proposed metal chaperone function of the *Re*NHase TG328-2 activator protein. CD data reveal a significant conformational change in the *Re*NHase TG328-2 activator protein occurs upon the addition of GTP. This conformational change may be linked to recognition and binding of the activator protein to the NHase α-subunit. A combination of these data establishes, for the first time, that the *Re*NHase TG328-2 activator protein falls into the COG0523 subfamily of G3E P-loop GTPases, a diverse group of GTPases with proposed roles in metal homeostasis, and that GTPase activity is regulated by metal binding.

Author Contribution

N.G. prepared expression plasmid, carried out protein expression, purification, enzymatic assays, prepared samples for metal analysis, analyzed the results, developed the homology model, and wrote the paper with R.C.H.; K.P.W.L. performed the ITC experiments. R.C.H. and B.B. conceived of the idea and wrote the paper with N.G. and K.P.W.L.

Funding

We thank the National Science Foundation [CHE-1412443, R.C.H. and CHE-1462201, B.B.] for funding this research.

Competing Interests

The Authors declare that there are no competing interests associated with the manuscript.

Abbreviations: ATP, adenosine triphosphate; CD, circular dichroism; EDTA, ethylenediaminetetraacetic acid; GTP, guanosine triphosphate; HEPES, 4-(2-hydroxyethyl)piperazine-1-ethanesulfonic acid; ICP-AES, inductively coupled plasma atomic emission spectroscopy; ITC, isothermal titration calorimetry; MBP, maltose-binding protein; NHase, nitrile hydratase; NTP, nucleoside

triphosphate; PDB, protein database; TCEP, tris(2-carboxyethyl)phosphine; TEV, tobacco etch virus; UTP, uridine triphosphate.

References

[1]Yamada, H. and Kobayashi, M. (1996) Nitrile hydratase and its application to industrial production of acrylamide. *Biosci. Biotech. Biochem.* 60, 1391–1400doi:10.1271/bbb.60.1391

[2]Brady, D., Beeton, A., Zeevaart, J., Kgaje, C., van Rantwijk, F., and Sheldon, R.A. (2004) Characterisation of nitrilase and nitrile hydratase biocatalytic systems. *Appl. Microbiol. Biotechnol.* 64, 76–85doi:10.1007/s00253-003-1495-0

[3]Kobayashi, M., Nagasawa, T., and Yamada, H. (1992) Enzymatic synthesis of acrylamide: a success story not yet over. *Trends Biotechnol.* 10, 402–408doi:10.1016/0167-7799(92)90283-2

[4]Nagasawa, T., Shimizu, H.,and Yamada, H. (1993) The superiority of the third-generation catalyst, Rhodococcus rhodochrous J1 nitrile hydratase, for industrial production of acrylamide. *Appl. Microbiol. Biotechnol.* 40, 189–195doi:10.1007/BF00170364

[5]Nagasawa, T., and Yamada, H. (1995) Interrelations of chemistry and biotechnology-VI. Microbial production of commodity chemicals. *Pure Appl. Chem.* 67, 1241–1256doi:10.1351/pac199567071241

[6]Prasad, S., and Bhalla, T.C. (2010) Nitrile hydratases (NHases): at the interface of academia and industry. *Biotechnol. Adv.* 28, 725–741doi:10.1016/j.biotechadv.2010.05.020

[7]Nagasawa, T., Mathew, C.D., Mauger, J., and Yamada, H. (1988) Nitrile hydratase-catalyzed production of nicotinamide from 3-Cyanopyridine in Rhodococcus rhodochrous J1. *Appl. Environ. Microbiol.* 54, 1766–1760 PMCID

[8]Kovacs, J.A., (2004) Synthetic analogues of cysteinate-ligated non-heme iron and non-corrinoid cobalt enzymes. *Chem. Rev.* 104, 825–848doi:10.1021/cr020619e

[9]Harrop, T.C., and Mascharak, P.K. (2004) Fe(III) and Co(III) centers with carboxamido nitrogen and modified sulfur coordination: lessons learned from nitrile hydratase. *Acc. Chem. Res.* 37, 253–260doi:10.1021/ar0301532

[10]Tsujimura, M., Odaka, M., Nakayama, H., Dohmae, N., Koshino, H., Asami, T., (2003) A novel inhibitor for Fe-type nitrile hydratase: 2-cyano-2-propyl hydroperoxide. *J. Am. Chem. Soc.* 125, 11532–11538doi:10.1021/ja035018z

[11]Dey, A., Chow, M., Taniguchi, K., Lugo-Mas, P., Davin, S., Maeda, M., (2006) Sulfur K-edge XAS and DFT calculations on nitrile hydratase:

geometric and electronic structure of the non-heme iron active site*. J. Am. Chem. Soc.* 128, 533–541doi:10.1021/ja0549695

[12]Nishiyama, M., Horinouchi, S., Kobayashi, M., Nagasawa, T., Yamada, H., and Beppu, T. (1991) Cloning and characterization of genes responsible for metabolism of nitrile compounds from Pseudomonas chlororaphis B23*. J. Bacteriol.* 173, 2465–2472 PMCID

[13]Hashimoto, Y., Nishiyama, M., Horinouchi, S., and Beppu, T. (1994) Nitrile hydratase gene from Rhodococcus sp. N-774 requirement for its downstream region for efficient expression*. Biosci. Biotechnol. Biochem.* 58, 1859–1865doi:10.1271/bbb.58.1859

[14]Nojiri, M., Yohda, M., Odaka, M., Matsushita, Y., Tsujimura, M., Yoshida, T., (1999) Functional expression of nitrile hydratase in Escherichia coli: requirement of a nitrile hydratase activator and post-translational modification of a ligand cysteine*. J. Biochem.* 125, 696–704doi:10.1093/oxfordjournals.jbchem.a022339

[15]Haas, C.E, Rodionov, D.A., Kropat, J., Malasarn, D., Merchant, S., and de Crecy-Lagard, V. (2009) A subset of the diverse COG0523 family of putative metal chaperones is linked to zinc homeostasis in all kingdoms of life*. BMC Genomics* 10, 470doi:10.1186/1471-2164-10-470

[16]Cameron, R.A., Sayed, M., and Cowan, D.A. (2005) Molecular analysis of the nitrile catabolism operon of the thermophile Bacillus pallidus RAPc8*. Biochim. Biophys. Acta* 1725, 35–46doi:10.1016/j.bbagen.2005.03.019

[17]Zhou, Z., Hashimoto, Y., Cui, T., Washizawa, Y., Mino, H., and Kobayashi, M. (2010) Unique biogenesis of high-molecular mass multimeric metalloenzyme nitrile hydratase: intermediates and a proposed mechanism for self-subunit swapping maturation*. Biochemistry* 49, 9638–9648doi:10.1021/bi100651v

[18]Zhou, Z., Hashimoto, Y., and Kobayashi, M. (2009) Self-subunit swapping chaperone needed for the maturation of multimeric metalloenzyme nitrile hydratase by a subunit exchange mechanism also carries out the oxidation of the metal ligand cysteine residues and insertion of cobalt*. J. Biol. Chem.* 284, 14930–14938doi:10.1074/jbc.M808464200

[19]Zhou, Z., Hashimoto, Y., Shiraki, K., and Kobayashi, M. (2008) Discovery of posttranslational maturation by self-subunit swapping*. Proc. Natl Acad. Sci. U.S.A.* 105, 14849–14854doi:10.1073/pnas.0803428105

[20]Cheng, T., Li, H., Yang, X., Xia, W., and Sun, H. (2013) Interaction of SlyD with HypB of Helicobacter pylori facilitates nickel trafficking*. Metallomics* 5, 804–807doi:10.1039/c3mt00014a

[21]Lu, J., Zheng, Y., Yamagishi, H., Odaka, M., Tsujimura, M., Maeda, M., (2003) Motif CXCC in nitrile hydratase activator is critical for NHase

biogenesis in vivo*. FEBS Lett.* 553, 391–396doi:10.1016/S0014-5793(03)01070-6

[22]Rzeznicka, K., Schätzle, S., Bottcher, D., Klein, J., and Bornscheuer, U.T. (2010) Cloning and functional expression of a nitrile hydratase (NHase) from Rhodococcusequi TG328-2 in Escherichia coli, its purification and biochemical characterisation*. Appl. Microbiol. Biotechnol.* 85, 1417–1425doi:10.1007/s00253-009-2153-y

[23]Donnelly, M.I., Zhou, M., Millard, C.S., Clancy, S., Stols, L., Eschenfeldt, W.H., (2006) An expression vector tailored for large-scale, high-throughput purification of recombinant proteins*. Prot. Expr. Purif.* 47, 446–454doi:10.1016/j.pep.2005.12.011

[24]Jancarik, J., Pufan, R., Hong, C., Kim, S.-H., and Kim, R. (2004) Optimum solubility (OS) screening: an efficient method to optimize buffer conditions for homogeneity and crystallization of proteins*. Acta Crystallogr. D Biol. Crystallogr.* D60, 1670–1673doi:10.1107/S0907444904010972

[25]Fusari, C., Demonte, A.M., Figueroa, C.M., Aleanzi, M., and Iglesias, A.A. (2006) A colorimetric method for the assay of ADP-glucose pyrophosphorylase*. Anal. Biochem.* 352, 145–147doi:10.1016/j.ab.2006.01.024

[26]Whitmore, L., and Wallace, B.A. (2004) DICHROWEB, an online server for protein secondary structure analyses from circular dichroism spectroscopic data*. Nucleic Acids Res.* 32, W668–W673doi:10.1093/nar/gkh371

[27]Whitmore, L., and Wallace, B.A. (2008) Protein secondary structure analyses from circular dichroism spectroscopy: methods and reference databases. *Biopolymers* 89, 392–400doi:10.1002/bip.20853

[28]Biasini, M., Bienert, S., Waterhouse, A., Arnold, K., Studer, G., Schmidt, T., (2014) SWISS-MODEL: modelling protein tertiary and quaternary structure using evolutionary information*. Nucleic Acids Res.* 42, 392–400doi:10.1093/nar/gku340

[29]Arnold, K., Bordoli, L., Kopp, J., and Schwede, T. (2006) The SWISS-MODEL workspace: a web-based environment for protein structure homology modelling*. Bioinformatics* 22, 195–201doi:10.1093/bioinformatics/bti770

[30]Bordoli, L., Kiefer, F., Arnold, K., Benkert, P., Battey, J., and Schwede, T. (2008) Protein structure homology modeling using SWISS-MODEL workspace*. Nat. Protoc.* 4, 1–13doi:10.1038/nprot.2008.197

[31]Guex, N., Peitsch, M.C., and Schwede, T. (2009) Automated comparative protein structure modeling with SWISS-MODEL and Swiss-PdbViewer: a historical perspective*. Electrophoresis* 30, S162–S173doi:10.1002/elps.200900140

[32]Laskowski, R.A., MacArthur, M.W., Moss, D.S., and Thornton, J.M. (1993) PROCHECK: a program to check the stereochemical quality of protein structures*. J. Appl. Crystallogr.* 26, 283–291doi:10.1107/S0021889892009944

[33]Eisenberg, D., Lüthy, R., and Bowie, J.U. (1997) [20] VERIFY3D: Assessment of protein models with three-dimensional profiles. In *Methods in Enzymology.* pp. 396–404, Academic Press

[34]Sydor, A.M., Jost, M., Ryan, K.S., Turo, K.E., Douglas, C.D., Drennan, C.L., (2013) Metal binding properties of Escherichia coli YjiA, a member of the metal homeostasis-associated COG0523 family of GTPases*. Biochemistry* 52, 1788–1801doi:10.1021/bi301600z

[35]Khil, P.P., Obmolova, G., Teplyakov, A., Howard, A.J., Gilliland, G.L., and Camerini-Otero, R.D. (2004) Crystal structure of the Escherichia coli YjiA protein suggests a GTP-dependent regulatory function*. Prot. Struct. Funct. Bioinfor. 54*, 371–374doi:10.1002/prot.10430

[36]Blaby-Haas, C.E., Flood, J.A., Crécy-Lagard, V.d., and Zamble, D.B. (2012) YeiR: a metal-binding GTPase from Escherichia coli involved in metal homeostasis*. Metallomics* 4, 488–497doi:10.1039/c2mt20012k

[37]Song, B.D., and Schmid, S.L. (2003) A molecular motor or a regulator? Dynamin's in a class of its own*. Biochemistry* 42, 1369–1376doi:10.1021/bi027062h

[38]Siderovski, D.P., and Willard, F.S. (2005) The GAPs, GEFs, and GDIs of heterotrimeric G-protein alpha subunits*. Int. J. Biol Sci.* 1, 51–66doi:10.7150/ijbs.1.51

[39]May, S.W., and Kuo, J.-Y. (1978) Preparation and properties of cobalt(II) rubredoxin*. Biochemistry* 17, 3333–3338doi:10.1021/bi00609a025

[40]Vasak, M., and Kagi, J.H. (1981) Metal thiolate clusters in cobalt(II)-metallothionein*. Proc. Natl Acad. Sci. U.S.A.* 78, 6709–6713doi:10.1073/pnas.78.11.6709

[41]Leipe, D.D., Wolf, Y.I., Koonin, E.V., and Aravind, L. (2002) Classification and evolution of P-loop GTPases and related ATPases*. J. Mol. Biol.* 317, 41–72doi:10.1006/jmbi.2001.5378